

New inorganic spinel oxides for use as negative electrode materials in future lithium-ion batteries

A.D. Robertson ^{a,*}, L. Trevino ^{a,b}, H. Tukamoto ^c, J.T.S. Irvine ^a

^a School of Chemistry, University of St. Andrews, UK

^b Facultad de Química, DES, UANL, Monterrey, Nuevo Leon, Mexico

^c GS Japan Storage Battery Company, Kyoto, Japan

Abstract

The electrochemical behaviour and associated structural changes of $\text{Li}_4\text{Ti}_5\text{O}_{12}$ have been investigated down to 0.01 V vs. Li/Li^+ . In addition, member of the solid solutions $\text{Li}_{1+x}\text{M}_{1-3x}\text{Ti}_{1+2x}\text{O}_4$, $\text{M} = \text{Fe}, \text{Ni}$ and Cr ($x = 0.30$) have been studied by a combination of electrochemical measurements and structural studies including neutron diffraction on as-prepared samples. © 1999 Elsevier Science S.A. All rights reserved.

Keywords: Titanate; Spinel; Li-ion battery; Neutron diffraction; Structure

1. Introduction

Present day lithium-ion cells typically comprise a lithiated carbon anode, organic liquid electrolyte and a lithium transition metal oxide cathode. These cells offer obvious advantages over nickel-cadmium and lead-acid cells i.e. superior energy density and low toxicity; however, there are still safety concerns regarding the carbon anode. A possibly safer alternative is to use solid state inorganic oxides as both the negative and positive electrode materials.

In 1994, Thackeray et al. demonstrated $\text{Li}_4\text{Ti}_5\text{O}_{12}$ spinel could be used as an electrode material in rechargeable lithium batteries [1]. The capacity is very stable with cycling; however, the voltage is rather high for utilisation as the negative electrode at more than 1.5 V vs. Li/Li^+ . The aim of the present study was to investigate the effect on the electrochemistry of $\text{Li}_4\text{Ti}_5\text{O}_{12}$ ($\equiv \text{Li}_{1.33}\text{Ti}_{1.67}\text{O}_4$) of replacing some of the Ti^{4+} by other 3d transition metals according to the substitution mechanism: $3\text{M}^{3+} \rightleftharpoons 2\text{Ti}^{4+} + \text{Li}^+$ where $\text{M}^{3+} = \text{Fe}^{3+}, \text{Ni}^{3+}, \text{Cr}^{3+}$. In particular, it was hoped that the working potential of 1.55 V vs. Li/Li^+ could be lowered. Blasse first reported the crystal chemistry of the Fe solid solution [2], although the electrochemical behaviour is not well known [3].

Fe is preferable over other transition metals such as Co and V due to its abundance and low toxicity. One possible disadvantage is the tendency for Fe^{3+} -containing spinels to be slightly inverse in character, i.e., some of the Fe^{3+} ions occupy the tetrahedral 8a sites as well as the 16d octahedral sites. It is generally believed that transition metals sharing the tetrahedral sites with the lithium ions in spinel oxides inhibit the lithium ions' diffusion through the lattice during intercalation and cause a decline in performance with repeated charge–discharge cycling. Ni and Cr were chosen as alternative dopants for this work given their similar ionic radii to Ti^{4+} and preference for octahedral coordination. The spinel LiCrTiO_4 is already known [4].

Results obtained from electrochemical and structural studies, including neutron diffraction, on all three solid solutions are presented.

2. Experimental

The starting reagents, Li_2CO_3 , Fe_2O_3 , NiO , Cr_2O_3 and TiO_2 (all Aldrich, > 99%) were dried overnight prior to use then weighed, mixed with ethanol, and ball-milled at room temperature for 30 min to ensure intimate mixing. Ball milling was also found to shorten reaction times and reduce firing temperatures, thereby minimising the risk of lithia loss. The powders were then dried and heated at 600–700°C for several hours and reground before firing at

* Corresponding author. Tel.: +44-1334-463814; Fax: +44-1334-463808; E-mail: adr1@st-and.ac.uk

900–1000°C for 1–2 h to complete reaction. Finally, samples were ball-milled again for a further 30 min.

For phase identification, a Philips PW1830 X-ray diffractometer with Cu K α radiation was used. Data were collected over the range $10^\circ \leq 2\theta \leq 70^\circ$. For lattice parameter determination, Si was used as an internal standard and data were collected up to $90^\circ 2\theta$ over several hours.

Powder neutron diffraction data were collected using the high resolution powder diffractometer (HRPD) situated at the ISIS neutron facility, Rutherford Appleton Laboratories, Didcot, Oxon, UK. Experiments were run at room temperature in a standard vanadium can for about 4h (800 μ A h). Time-of-flight data were collected between 2000 and 19550 μ s. Structural refinements were performed by the Rietveld method using the GSAS programme. Data greater than 11000 μ s were excluded from the final refinement as they contained information from the most intense reflection and were found to falsely skew the result.

For electrochemical testing, composite electrodes were prepared by suspending 75 wt.% active material, 10 wt.% super S carbon (to enhance electronic conductivity) and 15 wt.% poly(vinylidene fluoride) binder [Aldrich] in a fugitive solvent, such as cyclopentanone. The slurry was cast onto Cu foil and vacuum dried overnight at 75°C. Galvanostatic measurements were made using two electrode cells and a Macpile computerised battery test system. Li metal was used as the counter electrode and 1 molal LiPF₆ [Morita] in EC:DMC (1:2) [Grant Chemicals] as the electrolyte. The potential range was generally 0.01–2.00 V and the current density 0.1 mA cm⁻², equivalent to about C/10.

3. Results and discussion

Single-phase Li_{1.3}M_{0.1}Ti_{1.6}O₄ ($x = 0.30$) samples were prepared for each of the three solid solutions attempted, i.e., M = Fe, Ni and Cr. A complete range of solid solutions ($0.33 \leq x \leq -0.5$) exists for the Fe-containing system [2]. More extensive solid solutions may exist for the Ni-containing system but were not attempted during this study and LiCrTiO₄ ($x = 0.00$) is a known spinel [4].

3.1. Neutron refinement of Li_{1.3}M_{0.1}Ti_{1.6}O₄ (M = Fe, Ni, Cr)

The cation distribution in Li_{1.33}Ti_{1.67}O₄ is (Li)_{8a}(Li_{0.33}-Ti_{1.67})_{16d}O₄. To date, there has been no data published on neutron diffraction studies of admatal-modified Li_{1.33}Ti_{1.67}O₄. The main object of this experiment was to determine the relative positions and occupancies of the lithium, M, titanium and oxygen ions within the lattice.

Refinements of the data were carried out using the space group Fd-3 m (no. 227). The initial structural models comprised of lithium ions fully occupying the tetrahedral

8a sites, Ti, M and Li sharing the octahedral 16d sites (ratio 80:5:15) and O the 32e sites. The alternative cation sites: 8b, 16c and 48f were left unoccupied.

After varying the scale factor, unit cell dimensions and background coefficients, structural parameters were allowed to vary in the order (Ti, M), then oxygen, and finally Li. Isotropic temperature factors (ITFs) were then allowed to vary in the same order followed by the site occupancies. Refined models indicate that for M = Fe, all the Fe atoms co-occupy the tetrahedral 8a site with Li. For the Ni and Cr-containing compounds, however, M share the 16d octahedral site. Table 1 summarises the refined lattice parameters for the three compositions. Fig. 1 shows the fitted profile for Li_{1.3}Fe_{0.1}Ti_{1.6}O₄. Full details of the refined structures will be published elsewhere [5].

3.2. Electrochemical evaluation of Li_{1.33}Ti_{1.67}O₄ ($x = 0.33$)

The electrochemical behaviour of the M free end-member Li_{1.33}Ti_{1.67}O₄ has been studied already by previous authors [1,3,6–8]. On reduction there is a plateau at around 1.55 V vs. Li/Li⁺ corresponding to the two-phase coexistence of the initial spinel and a phase of stoichiometry Li_{2.33}Ti_{1.67}O₄. This reaction is completely reversible and on oxidation the extra mole of lithium can be removed and the original stoichiometry/cation distribution retained.

The mechanism is believed to involve the extra lithium ions occupying the vacant 16c sites in the spinel [1]. Simultaneously lithium ions in the tetrahedral 8a sites move into the remaining 16c sites due to electrostatic repulsion effects. The precise structure of the fully lithiated phase is not completely clear in the literature, either a rocksalt or a quasi-spinel depending on the amount of lithium ions that remain on the tetrahedral sites.

In order to investigate the possibility of additional plateaux at lower potentials, cells were cycled galvanostatically between 0.01 and 2.00 V. Fig. 2 shows the incremental capacity plot for the first three cycles. As expected, most capacity is in the region around 1.55 V, corresponding to the two-phase reaction outlined above. The expanded view shows that the position of the initial reduction peak is at a slightly lower potential than for subsequent cycles suggesting that there is an initial adaption of the structure to Li insertion, in agreement with previous authors [7]. In addition, there is an irreversible peak on initial reduction around 0.75 V vs. Li/Li⁺ and a reversible

Table 1
Cell parameters for Li_{1.3}M_{0.1}Ti_{1.6}O₄, refined from time-of-flight neutron diffraction data

Composition	a (Å)
Li _{1.3} Fe _{0.1} Ti _{1.6} O ₄	8.35867(4)
Li _{1.3} Ni _{0.1} Ti _{1.6} O ₄	8.35955(4)
Li _{1.3} Cr _{0.1} Ti _{1.6} O ₄	8.35407(3)

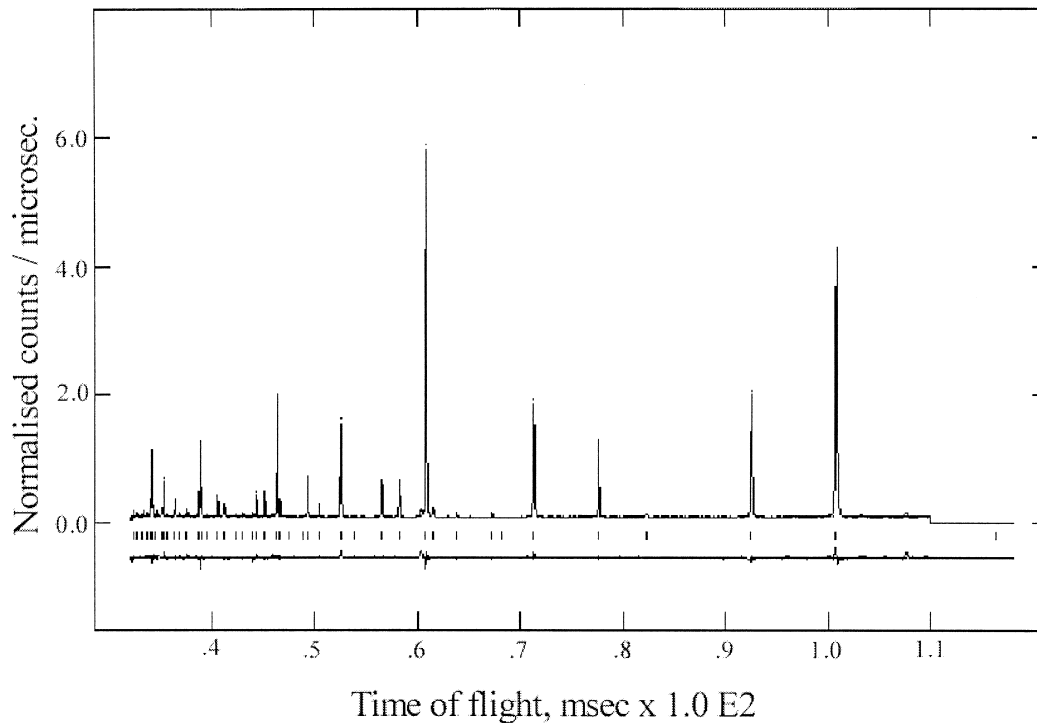


Fig. 1. Fitted profiles for refined $\text{Li}_{1.3}\text{Fe}_{0.1}\text{Ti}_{1.6}\text{O}_4$ time-of-flight neutron diffraction data. Tick marks indicate positions of expected Bragg reflections. Difference curves between observed and calculated patterns are shown below.

intercalation process occurring over a range of potentials < 0.60 V.

Analogous experiments with Super S carbon as the working electrode using identical potential range and cur-

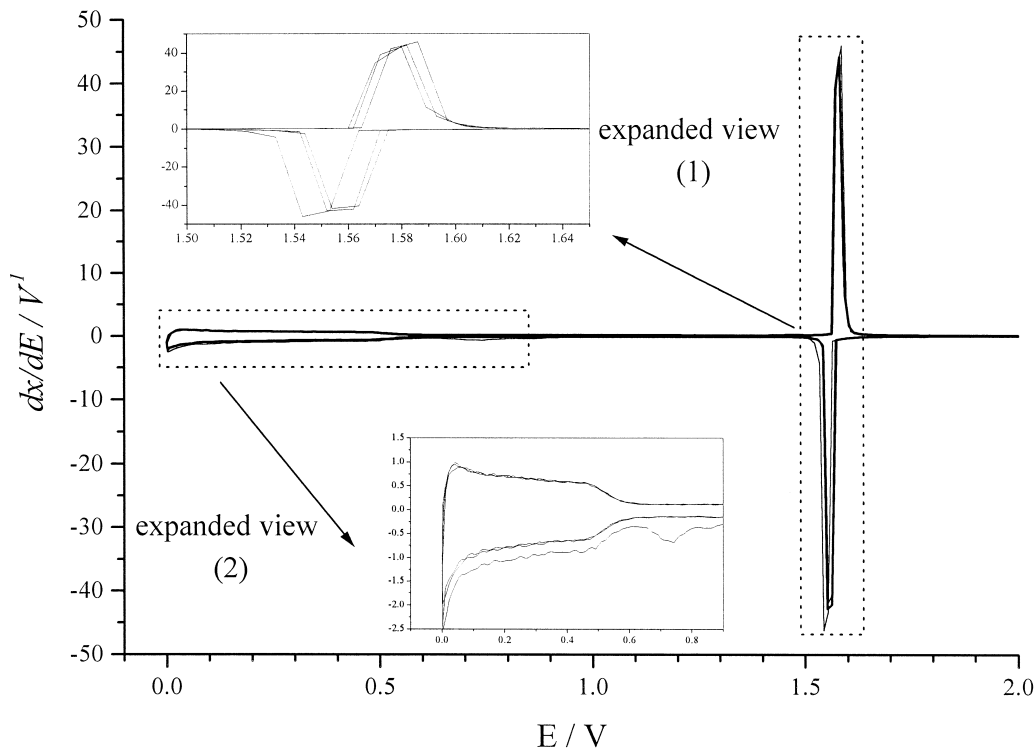


Fig. 2. Incremental capacity plot of the first three cycles for $\text{Li}_{1.33}\text{Ti}_{1.67}\text{O}_4$.

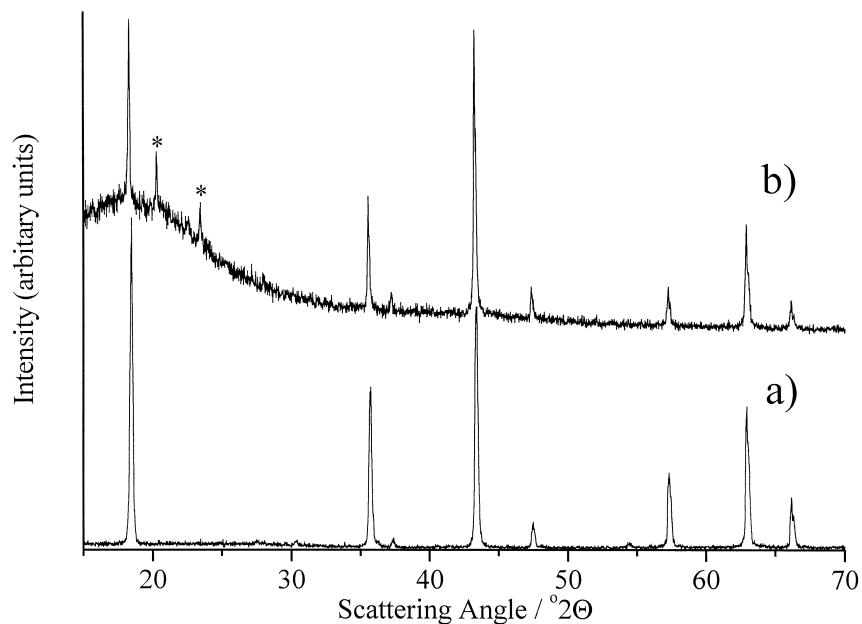


Fig. 3. X-ray diffraction patterns of (a) as-prepared and (b) fully lithiated (reduced to 0.2 V) $\text{Li}_{1.33}\text{Ti}_{1.67}\text{O}_4$.

rent density showed that the extra charge in the 0.75 V region for $\text{Li}_{1.33}\text{Ti}_{1.67}\text{O}_4$ is attributable to the initial passive film formation on the carbon and not due to the spinel. The other charge at low potentials cannot, however, be at-

tributed simply to the super S carbon and must in part be due to the titanate. The origin of the reactions at these potentials is not clear at this time but may include the (reversible) formation of anion deficient rocksalt species.

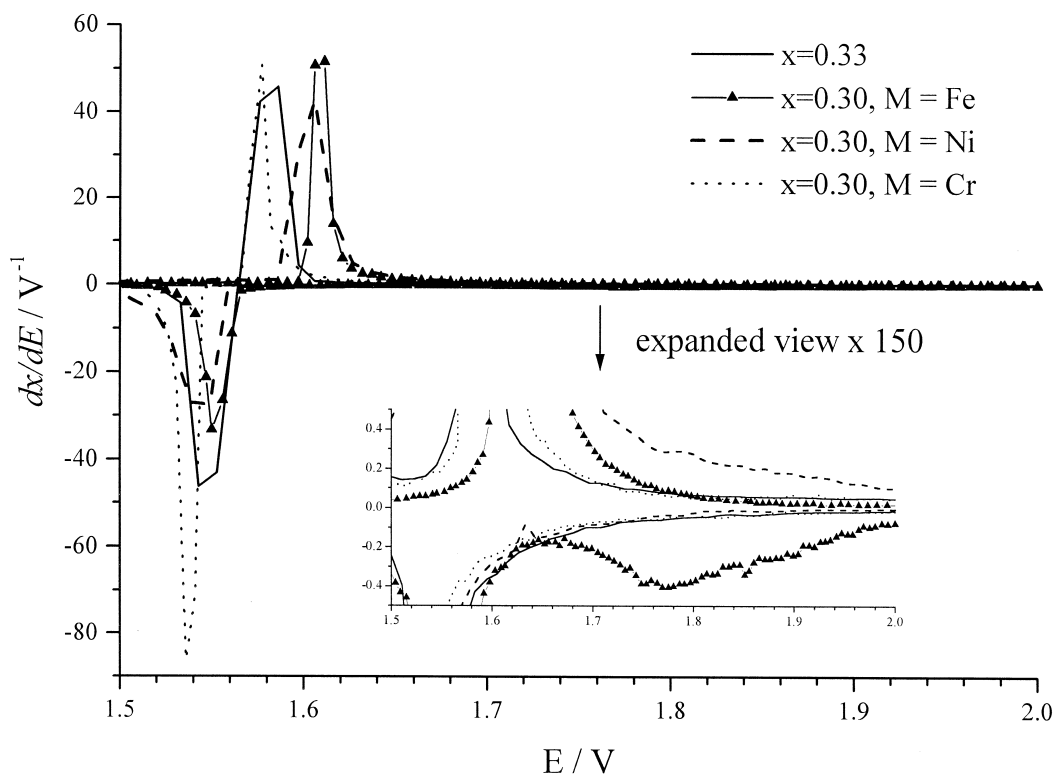


Fig. 4. Incremental capacity plot of the first cycle for $\text{Li}_{1.33}\text{Ti}_{1.67}\text{O}_4$ and $\text{Li}_{1.3}\text{M}_{0.1}\text{Ti}_{1.6}\text{O}_4$ ($\text{M} = \text{Fe}, \text{Ni}$ and Cr).

Table 2
Position of reduction/oxidation peaks shown in Fig. 4

	Position of peaks (V)		Difference between anodic and cathodic peak potentials: $\Delta_{\text{ox}} - \text{red}$ (V)
	Reduction	Oxidation	
$\text{Li}_{1.33}\text{Ti}_{1.67}\text{O}_4$	1.547	1.581	0.034
$\text{Li}_{1.3}\text{Fe}_{0.1}\text{Ti}_{1.6}\text{O}_4$	1.780, 1.552	1.609	0.057
$\text{Li}_{1.3}\text{Ni}_{0.1}\text{Ti}_{1.6}\text{O}_4$	1.543	1.604	0.061
$\text{Li}_{1.3}\text{Cr}_{0.1}\text{Ti}_{1.6}\text{O}_4$	1.538	1.576	0.038

Fig. 3 shows the X-ray diffraction patterns of (a) as-prepared and (b) fully lithiated (charged to 0.2 V) $\text{Li}_{1.33}\text{Ti}_{1.67}\text{O}_4$. The positions and relative intensities of the spinel peaks remain virtually unchanged after lithiation indicating that the general lattice framework is retained. There are, however, a couple of extra peaks at $2\theta = 20.28^\circ$ and 23.46° , presumably arising from the processes occurring below 0.8 V. X-ray diffraction patterns taken of fully lithiated super S carbon revealed no peaks in this region.

3.3. Electrochemical evaluation of $\text{Li}_{1.3}\text{M}_{0.1}\text{Ti}_{1.6}\text{O}_4$ ($M = \text{Fe}, \text{Ni}$ and Cr) solid solutions.

Fig. 4 shows the first cycle incremental capacity plots for $\text{Li}_{1.3}\text{M}_{0.1}\text{Ti}_{1.6}\text{O}_4$ ($M = \text{Fe}, \text{Ni}$ and Cr) and $\text{Li}_{1.33}\text{Ti}_{1.67}\text{O}_4$ over the potential range 1.5–2.0 V. For all three admatal-modified compositions the difference in the main reduction/oxidation peak potentials is greater than that observed with $\text{Li}_{1.33}\text{Ti}_{1.67}\text{O}_4$, Table 2. However, for $M = \text{Cr}$,

the potentials are lower on reduction and oxidation compared with undoped lithium titanate spinel and the peaks appear sharper. Capacity in this potential range is also slightly higher for the Cr-doped sample; 1.04 moles of lithium can be inserted reversibly as opposed to 1 mole for $\text{Li}_{1.33}\text{Ti}_{1.67}\text{O}_4$. This is an interesting point as normally spinels can only reversibly insert 1.00 mole of lithium ions and needs to be investigated further. These deviations in electrochemical behaviour observed for the Cr-modified spinel may be a result of the Cr being reduced in addition to Ti although further work, perhaps on compositions containing more Cr, will be required to confirm this.

It is also interesting to note that for $M = \text{Fe}$, there is an additional slight peak around 1.78 V on reduction presumably associated with $\text{Fe}_{(8a)}^{3+} - \text{Fe}^{2+}$. There is no corresponding peak on oxidation up to 2.00 V although higher potentials may be required.

Fig. 5 shows the anodic capacity as a function of cycle number for all four compositions over the whole potential range, i.e., 0.01–2.00 V. By assuming that the Super S carbon simply enhances the electronic conductivity of the composite electrode material and there is no reaction between it and the spinel, it is possible to subtract the capacity of the Super S from the total capacity observed. Even allowing for this correction, the capacity values for $\text{Li}_{1.33}\text{Ti}_{1.67}\text{O}_4$ and $M = \text{Ni}, \text{Cr}$ are about 40 mA h g^{-1} in excess of the theoretical $170\text{--}175 \text{ mA h g}^{-1}$ expected for the removal of 1 mole of lithium ions. This excess capacity is associated with the very broad region of extra charge at $< 0.6 \text{ V}$ observed in the dx/dE plots and, as stated above, the precise nature of the reactions occurring are not

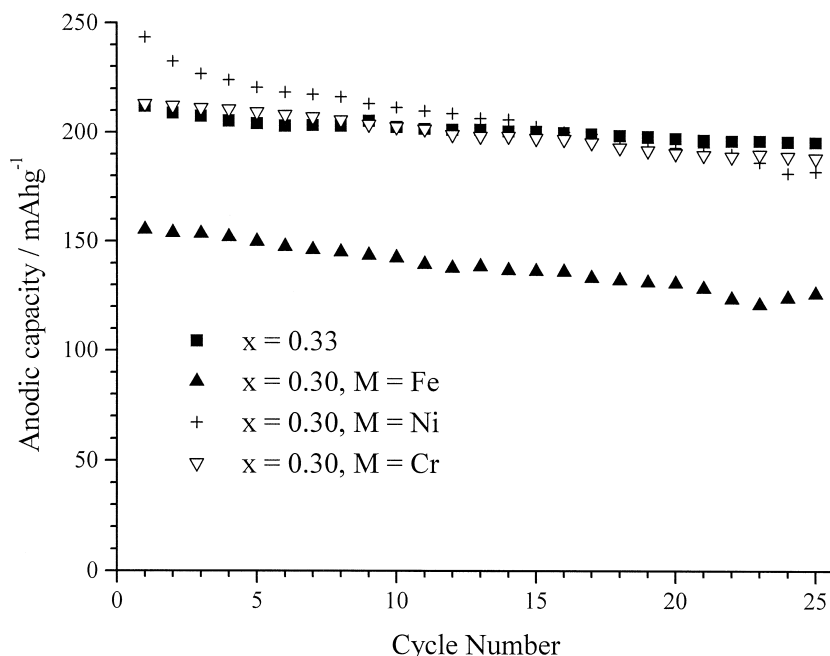


Fig. 5. Anodic capacity as a function of cycle number for $\text{Li}_{1.33}\text{Ti}_{1.67}\text{O}_4$ and $\text{Li}_{1.3}\text{M}_{0.1}\text{Ti}_{1.6}\text{O}_4$ ($M = \text{Fe}, \text{Ni}$ and Cr), corrected for Super S. $V_{\text{limits}} = 0.01\text{--}2.00 \text{ V}$, $i = 0.1 \text{ mA}$. One molal LiPF_6 in EC:DMC (1:2) electrolyte.

yet understood. The capacity in this region is greatest for $M = \text{Ni}$, however, the difference in capacities between anodic and cathodic processes in this region are quite large throughout cycling, indicating irreversible reactions take place beyond the first cycle. Capacity fade is also greatest for $M = \text{Ni}$.

4. Conclusions

The electrochemical behaviour of $\text{Li}_4\text{Ti}_5\text{O}_{12}$ has been modified by the addition of a small amount of admatal according to the substitution mechanism $3\text{M}^{3+} \leftrightarrow 2\text{Li}^+ + \text{Ti}^{4+}$. The potential of the main reduction peak was reduced by 0.09 V for $M = \text{Cr}$, and this system seems the most promising. The precise mechanism of intercalation is still unclear and further structural studies such as neutron refinement or solid state NMR on material at various stages of charge and discharge are planned to determine the cation distribution in the lithiated phases.

Acknowledgements

The authors would like to thank the GS Japan Storage Battery Company for funding.

References

- [1] E. Ferg, R.J. Gummow, A. de Kock, M.M. Thackeray, J. Electrochem. Soc. 141 (1994) L147.
- [2] G. Blasse, Philips Res. Rep. 20 (1965) 528.
- [3] P. Birke, S. Döring, S. Scharner, W. Weppner, Ionics 2 (1996) 329.
- [4] M.A. Arillo, M.L. Lopez, M.T. Fernandez, M.L. Veiga, C. Pico, J. Solid State Chem. 125 (1996) 211.
- [5] A.D. Robertson, J.R.T. Tolchard, L. Trevino, H. Tukamoto, J.T.S. Irvine, in preparation.
- [6] T. Ohzuku, A. Ueda, N. Yamamoto, Y. Iwakoshi, J. Power Sources 54 (1995) 99.
- [7] T. Ohzuku, A. Ueda, N. Yamamoto, J. Electrochem. Soc. 142 (1995) 1431.
- [8] S. Sarciaux, A.L.G. La Salle, D. Guyomard, Y. Piffard, Proceedings of ISIC 9, Arcachon, France, May 1997.